Journal of *Marine Science and Engineering*

MDPI

Article

Investigating Spatial Distribution of Green-Tide in the Yellow Sea in 2021 Using Combined Optical and SAR Images

Yufei Ma [1], Kapo Wong [2], Jin Yeu Tsou [3] and Yuanzhi Zhang [1,3,*]

[1] School of Marine Sciences, Nanjing University of Information Science and Technology, Nanjing 210044, China; 20201237008@nuist.edu.cn
[2] School of Nursing, The Hong Kong Polytechnic University, Hong Kong 999666, China; portia.wong@polyu.edu.hk
[3] Center for Housing Innovations, Institute of Asia-Pacific Studies, Faculty of Social Science, Chinese University of Hong Kong, Hong Kong 999777, China; jytsou@cityu.edu.hk
* Correspondence: yuanzhizhang@cuhk.edu.hk; Tel.: +852-6995-2064

Abstract: Optical remote sensing is limited to clouds and rain. It is difficult to obtain ground object images in severe weather. Microwave remote sensing can penetrate clouds and rain to obtain ground object images. Therefore, this paper combines optical and microwave data to analyze the time and space of the green-tide in the Yellow Sea in 2021. Compared with a single data source, the distribution characteristics increase the frequency of time observation and show the green-tide changes in more detail. The continuous remote sensing observation time is 80 days. *Ulva prolifera* has experienced discovery (mid-late May), development (mid-late May to early June), outbreak (early June to mid-late June), decline (late June to mid-July), and extinction (late July to mid-August) in five stages; the development period drifts along the northeast direction, the outbreak period drifts along the northwest direction, the decline and extinction periods are mainly in the Rizhao and Qingdao waters. *Ulva prolifera* has a tendency to drift northward as a whole, drifting through Yancheng, Lianyungang, Linyi, Rizhao and Qingdao waters eventually landing on the coast of Qingdao and gradually disappearing.

Keywords: green-tide; MODIS; SAR; Southern Yellow Sea; spatiotemporal variation

Citation: Ma, Y.; Wong, K.; Tsou, J.Y.; Zhang, Y. Investigating Spatial Distribution of Green-Tide in the Yellow Sea in 2021 Using Combined Optical and SAR Images. *J. Mar. Sci. Eng.* **2022**, *10*, 127. https://doi.org/10.3390/jmse10020127

Academic Editor: Stefano Vignudelli

Received: 4 December 2021
Accepted: 12 January 2022
Published: 19 January 2022

1. Introduction

Green-tide is an abnormal ecological phenomenon caused by the macroalgae in the seawater that multiply or gather under certain environmental conditions. In 2007, green tides were first discovered in the central and northern parts of the Yellow Sea in China. The main species of green tide algae in the Yellow Sea are *Ulva prolifera* [1,2]. Since then, green tide disasters have erupted in the Yellow Sea from May to July every year, severely affecting the aquaculture, coastal tourism, and maritime transportation industries in coastal cities and destroying the marine ecosystem [3,4].

The origin of the Yellow Sea's green-tide is not yet clear, and there are four main points of view. The first point of view is that *Ulva prolifera* yellow sea came from animal breeding ponds along the southern coast of the Yellow Sea because the green algae in this pond and Qingdao floating green algae belong to *Ulva prolifera* species [5,6]. The second point of view is that *Ulva prolifera* came from the southern Shandong peninsula to the north side of the Yangtze River estuary from the salt ponds, aquaculture ponds, canals and water channel inlets, estuaries and sea gates, beaches and sandbar laver cultivation areas and other green algae distribution areas [7]. The third point of view is that the source of the *Ulva prolifera* yellow sea is from the bottom of the sea because part of the green tide of the previous year will sink to the bottom of the sea [8]. The fourth point of view is the most widely accepted. It believes that *Ulva prolifera* yellow sea comes from the raft culture area in the southern part of the Yellow Sea. In mid-April, the laver cultivation area began to recycle the cultivation

tools. The green algae are easy to attach to the stem rope of the fixed raft. When the tide is high, the cleaned green algae enter the sea with the tide [9–11].

Green tide outbreaks last for a long time and have a wide range. Traditional monitoring methods such as ships and airplanes have limited observation ranges, which consume a lot of manpower, material resources and time. Satellite remote sensing technology can obtain the time and range of *Ulva prolifera* outbreaks in real-time, intuitively providing reliable scientific and technological support for the government's disaster prevention and mitigation emergency departments [12].

MODIS (Moderate-resolution Imaging Spectroradiometer) data have a wide range of bands, a wide acquisition range, a fast update frequency, and are free and easy to obtain. They are the most commonly used data in *Ulva prolifera* remote sensing monitoring [13]. During the 2008 Beijing Olympic Games, the Yellow Sea experienced a severe outbreak of *Ulva prolifera*. Hu et al. [14] used MODIS data for the first time to analyze the origin, marine distribution and temporal changes of *Ulva prolifera*. During the outbreaks of *Ulva prolifera* in 2013, 2015 and 2018, MODIS data were also applied to the monitoring of *Ulva prolifera* [15–17]. GOCI (Geostationary Ocean Color Imager) is the world's first geostationary satellite for ocean color observation. Its high coverage and high time resolution provide a sufficient data guarantee for *Ulva prolifera* remote sensing. Song Debin et al. [18] and Chen Ying et al. [19] combined GOCI data to study the evolution and drift path of *Ulva prolifera* in 2017. Compared with MODIS and GOCI data, HuanJing (HJ)–CCD (Charge-Coupled Device) has a higher spatial resolution. The research is based on HJ-CCD data, using the classical vegetation index algorithm and the artificial assisted interpretation method, and analyzing the distribution and drift route of the *Ulva prolifera* process in 2013 [20].

The extraction algorithm of *Ulva prolifera* based on the optical sensor generally uses the band ratio method. The Normalized Vegetation Index (NDVI) and Enhanced Vegetation Index (EVI) were initially used to map global vegetation and terrestrial primary productivity. Since the green tide is close to the reflection characteristics of terrestrial vegetation, it has strong absorption characteristics in the visible red band, and there are reflection peaks in the near-infrared band. These two vegetation indices have begun to be applied to the extraction of *Ulva prolifera* [21–23]. NDVI is more sensitive to low-vegetation areas and is helpful for early and mid-term detection of *Ulva prolifera* [24,25]. However, the NDVI method is susceptible to changes in the atmospheric conditions, observation angles, sun angles and the marine environment during satellite observations. There are uncertainties in the monitoring of algae. Hu et al. [26] proposed the floating algae index method (FAI). FAI reduces the sensitivity to the environment and observation conditions and is more accurate and stable than the NDVI method. However, there is still significant uncertainty, and it is more suitable for high-resolution images. The FAI index requires images in the short-wave infrared band, but images such as HJ-1 lack this band, so Xing and Hu [27] proposed a floating algae index based on virtual baseline height (VB-FAH). Shi et al. [28] proposed the normalized algae index method (NDAI), which removes the atmosphere's influence on the interpretation results compared with the NDVI method.

Under normal circumstances, the backscattering of radar waves by green tides is stronger than seawater's backscattering of radar waves, which provides a theoretical basis for microwave inversion of green tide information. Achille Ciappa et al. [29] used ScanSAR (COSMO-SkyMed) data to monitor *Ulva prolifera* offshore Qingdao from July 14–18 2008. Jiang Xingwei et al. [30] used SAR (COSMO-SkyMed) data to extract information about *Ulva prolifera* in 2008, and the extraction method was based on region-growing object-oriented image scale segmentation. Shen et al. [31] proposed a new green tide extraction index for RADARSAT-2 SAR images to distinguish between seawater and *Ulva prolifera*, and realized unsupervised detection.

Although optical remote sensing can provide a wealth of color information, the received sea surface satellite image will be blocked by clouds and rain and cannot obtain green tide information. Microwave remote sensing can make up for this deficiency, and it can penetrate clouds and rain imaging. At the same time, the number of optical images in sunny weather is

small, and microwave data can further supplement the data and increase the frequency of time monitoring. Therefore, this paper uses a combination of optical data MODIS (Moderate-resolution Imaging Spectroradiometer) and microwave data Synthetic Aperture Radar (SAR, Sentinel-1A/B) to study the spatiotemporal changes of the green tide.

2. Materials and Methods

2.1. Study Area and Data

The Yellow Sea (31°40′ N–39°50′ N, 119°10′ E–126°50′ E) is a shallow half-closed continental shelf, located in the western Pacific Ocean, between the Chinese mainland and the Korean peninsula, the northwest is connected to the Bohai Sea, and the south is connected to the East China Sea. The connection between Chengshanjiao at the eastern end of the Shandong Peninsula and Changshan on the Korean Peninsula can divide the Yellow Sea into the South Yellow Sea and the North Yellow Sea. The South Yellow Sea is the main area where green tides erupt. This area was taken as the study area, in which the range is determined to be 31° N–37° N, 119° E–124° E (Figure 1). The north or northeast wind prevails in the southern part of the Yellow Sea in winter, and the south–southeast wind prevails in summer. The cloud cover over the southern part of the Yellow Sea increases significantly, and there is a cloudy zone. There are economically developed cities along the Yellow Sea, such as Qingdao, Rizhao, Lianyungang, and Yancheng. The land runoff into the sea carries rich inorganic nutrients, providing conditions for the explosive growth of green tide algae.

The research data include optical data and microwave data (Table 1), which come from MODIS (TERRA/AQUA) and SAR (Sentinel-1A/B), respectively. MODIS has a wide scanning range, reaching 2330 km, with high time resolution, and the revisit period is only one day. It has three spatial resolutions of 250 m, 500 m and 1 km, suitable for large-scale green tide monitoring. The spectrum of MODIS ranges from visible light to thermal infrared, divided into 36 channels. The spatial resolution of the first two channels is 250 m, including the red light band and the near-infrared band. The spatial resolution of channels 3–7 is 500 m, and the spatial resolution of channels 8–36 is 1 km. This article selects MODIS L1 B 250 m spatial resolution data, calibrated by the instrument and contains geographic coordinate information, and stores reflectance and emissivity. Sentinel-1 consists of two polar-orbiting satellites, A and B, which are equipped with C-band synthetic aperture radar (SAR); it has four imaging modes, including Stripmap (SM), Interferometric Wide swath (IW), Extra Wide swath (EW) and Wave mode. Sentinel-1 data are distributed through Level-0, Level-1, and Level-2. Level-1 products have two types: Single Look Complex (SLC) and Ground Range Detected (GRD). GRD data are the focus data of SLC data after multi-view processing, using WGS84 ellipsoid projection to the ground distance. This article selects the Level-1 product that is imaged in the IW mode and determines the GRD type. This product has VV and VH polarization methods. Because the contrast between *Ulva prolifera* and seawater is more obvious in the images generated by the VV polarization method, the image generated by the VV polarization is preferred. The IW mode uses a medium resolution, and the acquisition width is 250 km. The SAR data have high spatial resolution and are not affected by weather and climate, making up for the lack of optical data monitoring under cloud conditions. The download address of MODIS data is Find Data–LAADS DAAC (nasa.gov, accessed on 20 September 2021), screening eight scenes of cloudless or less clouded images in the South Yellow Sea from May to July 2021. The download address of the SAR data is Ocean Virtual Laboratory (oceandatalab.com, accessed on 20 September 2021), which screens 18 images that continuously cover the South Yellow Sea from May to July 2021 (at least three images are required to cover the study area every day).

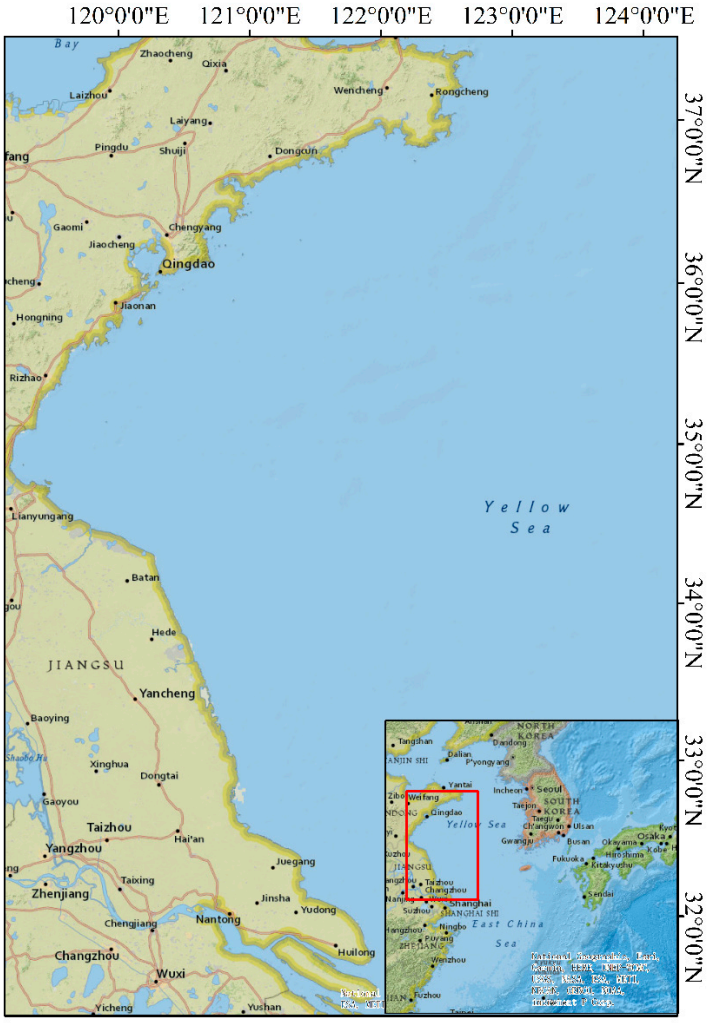

Figure 1. The study area (red rectangle showing the area of green tide).

Table 1. Main data sources and products.

Satellite	Sensor	Resolution/m	Band	Product	Revisit Cycle/d
TERRA/AQUA	MODIS	250	red/near-infrared	L1-B	1
Sentinel-1A/B	SAR	5 × 20	C	L1-GRD (VV)	12
Data Time					
Optics	24/5/2021 25/5/2021 28/5/2021 4/6/2021 5/6/2021 6/6/2021 19/6/2021 23/6/2021				
Microwave	31/5/2021 12/6/2021 18/6/2021 30/6/2021 12/7/2021 24/7/2021 5/8/2021 11/8/2021				

2.2. Research Methods and Data Processing

2.2.1. MODIS Image Preprocessing

The steps of using MODIS images to extract *Ulva prolifera* are shown in Figure 2. Due to the radiation distortion, geometric distortion, atmospheric interference and other influencing factors in the original MODIS image (Figure 3a), it was first preprocessed in the ENVI (The Environment for Visualizing Images) software 5.3. For MODIS 02 level data, ENVI will automatically complete the calibration of the data when opening the data, and then use the satellite's own geolocation file to perform geometric correction to eliminate the geometric distortion and "butterfly effect" of the MODIS data. Then the data were cut according to the scope of the study area, and finally the FLAASH correction tool (Fast

Line-of-sight Atmospheric Analysis of Spectral Hypercubes) was used in ENVI to perform atmospheric correction on the image. FLAASH is based on the MODTRAN4+ radiation transmission model. The input file of the FLAASH module is the radiance value, the file type is BIL or BIP, and the data header file contains the center wavelength. In order to change the unit and data type of the input radiance value to a floating-point radiance value of μW/(cm^2•nm•sr), the conversion coefficient of MODIS data was set to 10. Then, according to the image, information such as the latitude and longitude of the image center, the sensor type, the average altitude of the image area, the image pixel size, the imaging date and the imaging time are set. This paper selects the MODTRAN atmospheric model based on the season/latitude, the Sub-Arctic Summer model for the MODIS images in May, and the Mid-Latitude Summer model for the MODIS images in June and July. The urban is selected for the aerosol model, and the K-T aerosol inversion method is used. In the multi-spectral setting, the KT uplink channel selects the near-infrared band, and the KT downlink channel selects the red light band. In FLAASH advanced settings, adjacency correction is not used. After setting all the parameters, the atmospheric correction of the MODIS image is completed. Finally, the projection of each image is converted to the WGS_1984_UTM_Zone_51N projection coordinate system. The MODIS image after preprocessing is shown in Figure 3b, and some *Ulva prolifera* is seen on the sea surface.

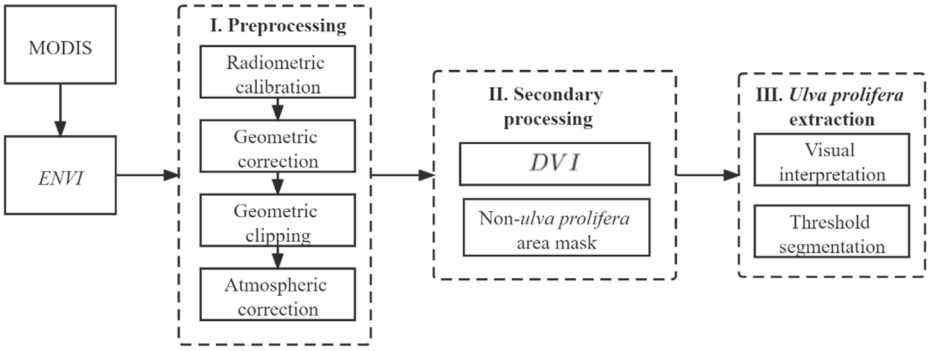

Figure 2. Flow chart of MODIS image preprocessing.

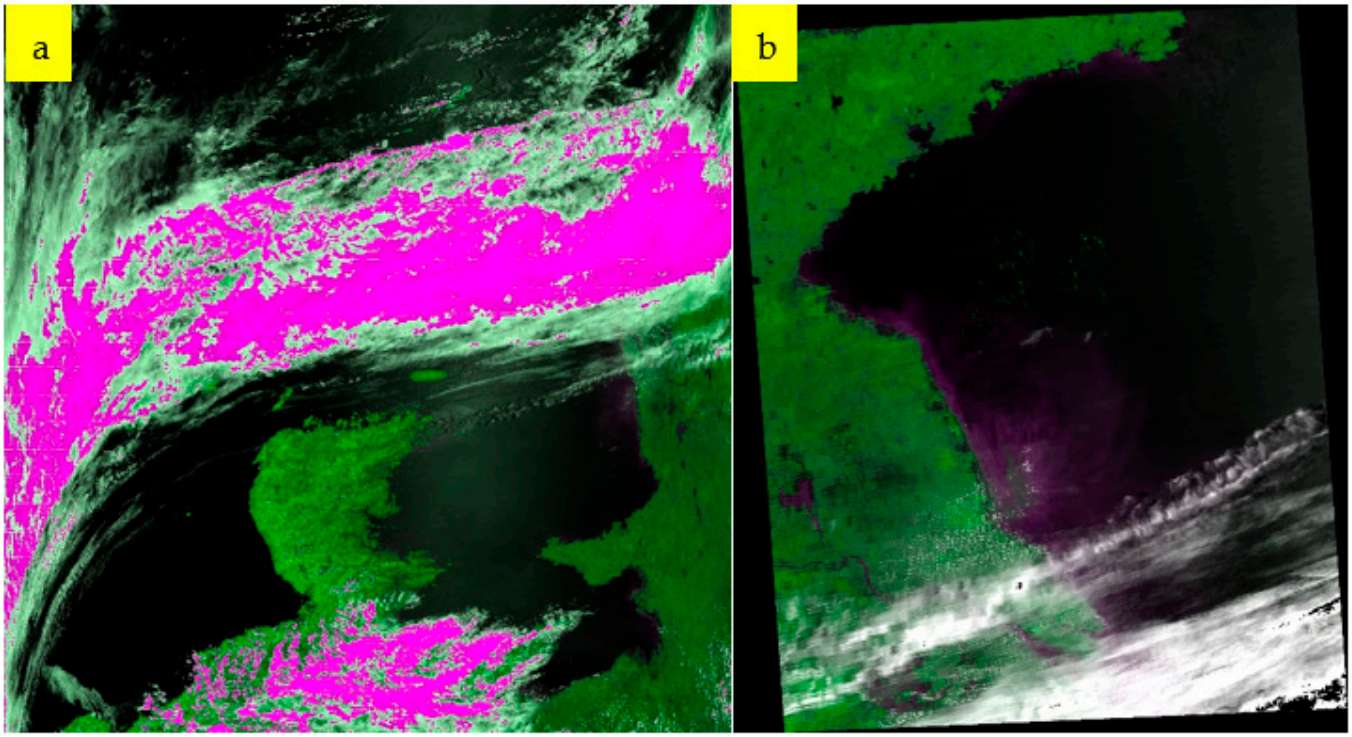

Figure 3. MODIS false color image on 4 June 2021. (**a**) MODIS image without pre-processing; (**b**) MODIS image with pre-processing.

2.2.2. *Ulva prolifera* Extraction Based on MODIS Images

Ulva prolifera has reflection characteristics similar to vegetation, visible light reflectivity but low near-infrared reflectivity, and difference vegetation index (such as DVI, FAI) is a commonly used vegetation index algorithm, which is less sensitive to the effects of sunlight and aerosol changes. MODIS L1 B data only contain red (Red) and near-infrared (NIR) bands, so this article uses the DVI algorithm.

$$DVI = R_{nir} - R_r$$

In the formula, *DVI* is the difference vegetation index value of the image, and R_{nir} and R_r are the ground object reflectivity of the image in the near-infrared waveband and red light waveband, respectively. The image after *DVI* processing is shown in Figure 4.

Because *Ulva prolifera* has image features similar to vegetation, directly using the MODIS image shown in Figure 4 to extract *Ulva prolifera* can easily misclassify the vegetation into *Ulva prolifera*. Therefore, this article masks the land and only retains *Ulva prolifera* and sea water, as shown in the red frame area in Figure 4. In order to extract the *Ulva prolifera* information, a reasonable DVI threshold is set in combination with the false color image, and the optimal threshold is selected for visual judgment. The result of *Ulva prolifera* extracted by the optimal threshold should coincide with the *Ulva prolifera* region in the image. After repeated comparisons, the optimal threshold of MODIS images on 4 June 2021 is 0.03, and the extraction results are shown in Figure 5.

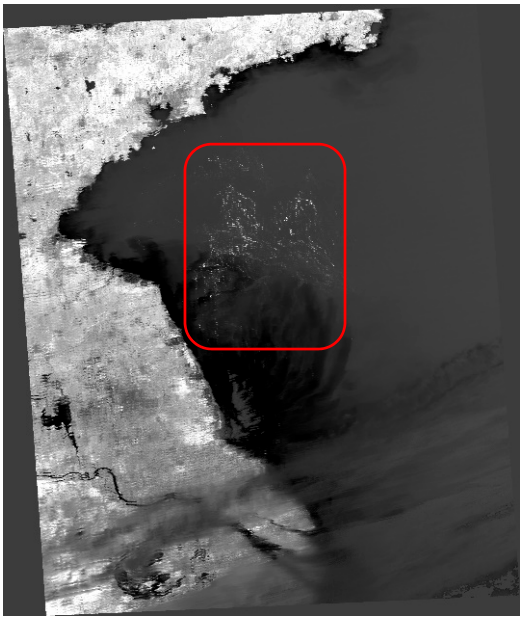

Figure 4. MODIS image on 4 June 2021 after DVI processing.

Figure 5. The extraction results of *Ulva prolifera*.

2.2.3. SAR Image Preprocessing

The width of the SAR image is 250 km, and at least three images are required to cover the South Yellow Sea area (Figure 4). Figure 5 is a VV image of the SAR L1 GRD mode in the South Yellow Sea region on 12 July 2021. The three images correspond to the regions a, b, and c in Figure 4, respectively. The SAR image has geometric distortion, radiation distortion and noise interference (Figure 5). This article uses SNAP (Sentinel Application Platform) software 8.0 to preprocess it. The preprocessing steps include orbit correction, thermal noise removal, radiation calibration, coherent speckle filtering, terrain correction, decibelization and mosaic (Figures 6 and 7, respectively). The preprocessed flowchart and image are shown in Figures 8 and 9, respectively.

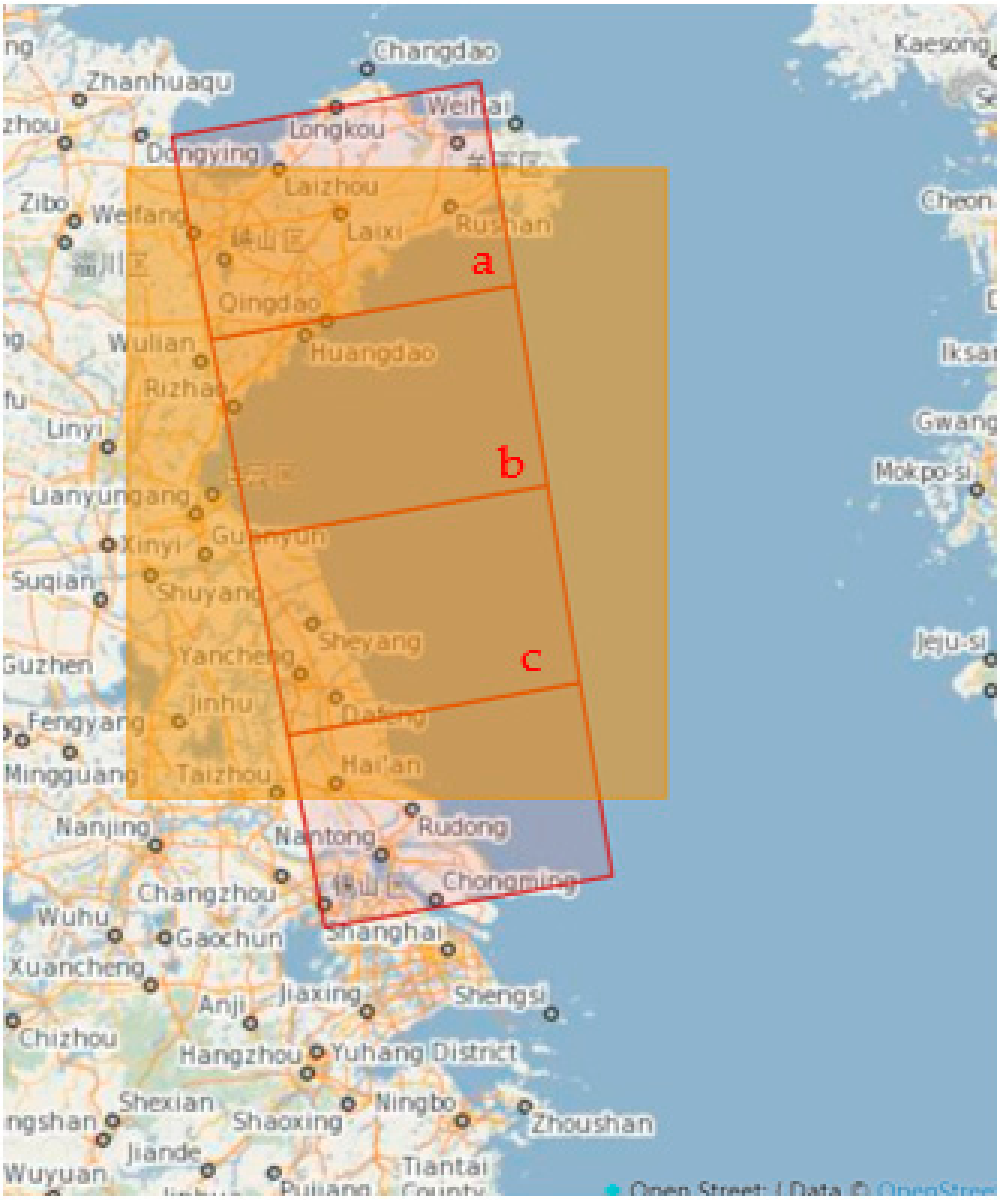

Figure 6. SAR image distribution in the South Yellow Sea. (**a**) Qingdao, (**b**) Rizhao and Liangungang, and (**c**) Yancheng and Nantong.

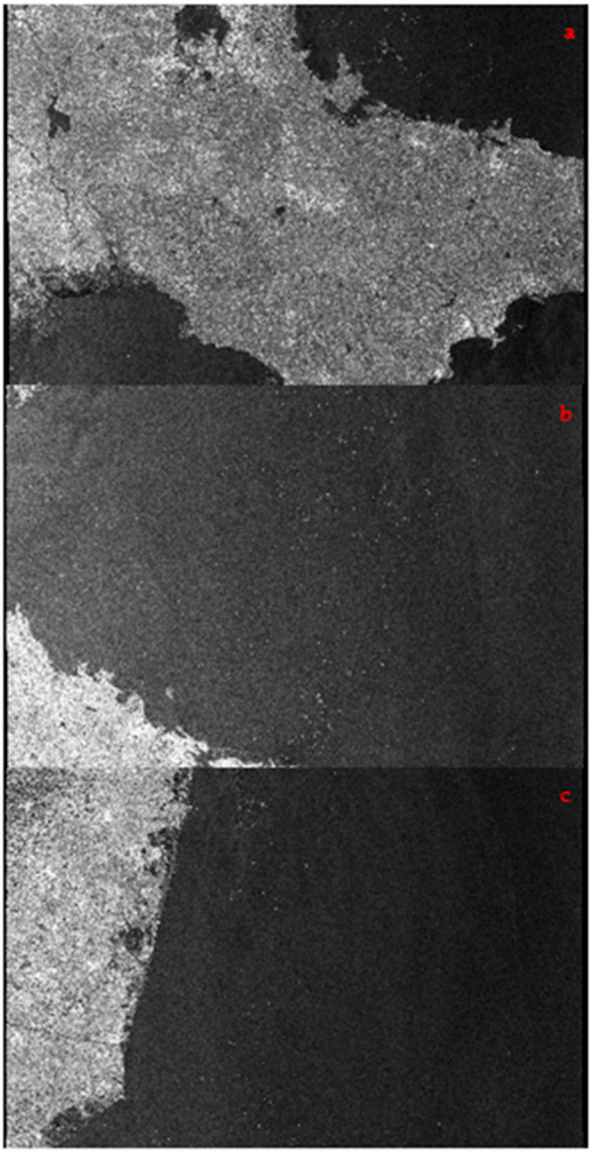

Figure 7. SAR image of the South Yellow Sea area on 12 July 2021. (**a**) Qingdao, (**b**) Rizhao and Liangungang, and (**c**) Yancheng and Nantong.

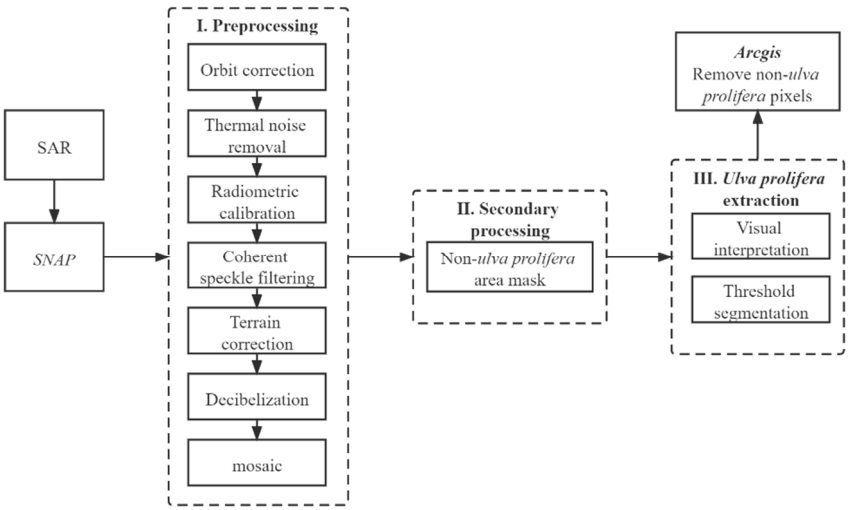

Figure 8. SAR image preprocessing flow chart.

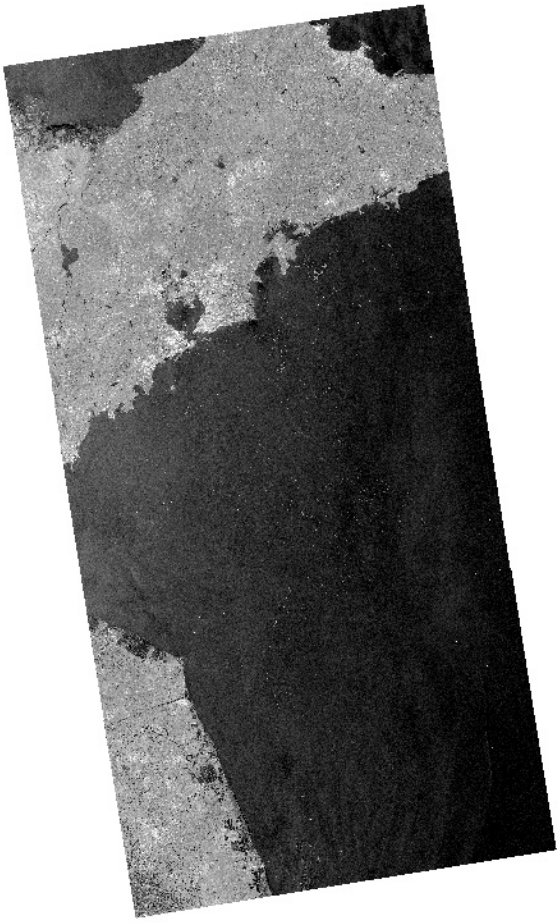

Figure 9. The SAR image of the South Yellow Sea area on 12 July 2021 after preprocessing.

2.2.4. *Ulva prolifera* Extraction Based on SAR Images

Before extracting *Ulva prolifera*, the SAR image was masked by land. After visual interpretation and dynamic threshold selection, it was determined that the optimal threshold for extracting *Ulva prolifera* was −15 dB. Figure 9 shows the results of *Ulva prolifera* extraction. In addition to *Ulva prolifera* pixels, the extraction results also contain fine spots, coherent speckle noise, splicing lines between images, land-coast pixels, ships, and coastal aquaculture areas (Figures 10 and 11).

In order to remove non-*ulva prolifera* pixels, the result image shown in Figure 7 was imported into ArcGIS, first converted to vectors, and then fused to reduce scattered patches, but there were still a large number of finely-fragmented non-enteross patches in the image. The area of all patches was counted and they were sorted in ascending order, and the fine patches with an area less than 0.01 km^2 were deleted. After that, non-*ulva prolifera* pixels, such as ships, noises, breeding areas, coastal land features, and so forth, were manually deleted. The final extraction result is shown in Figure 12.

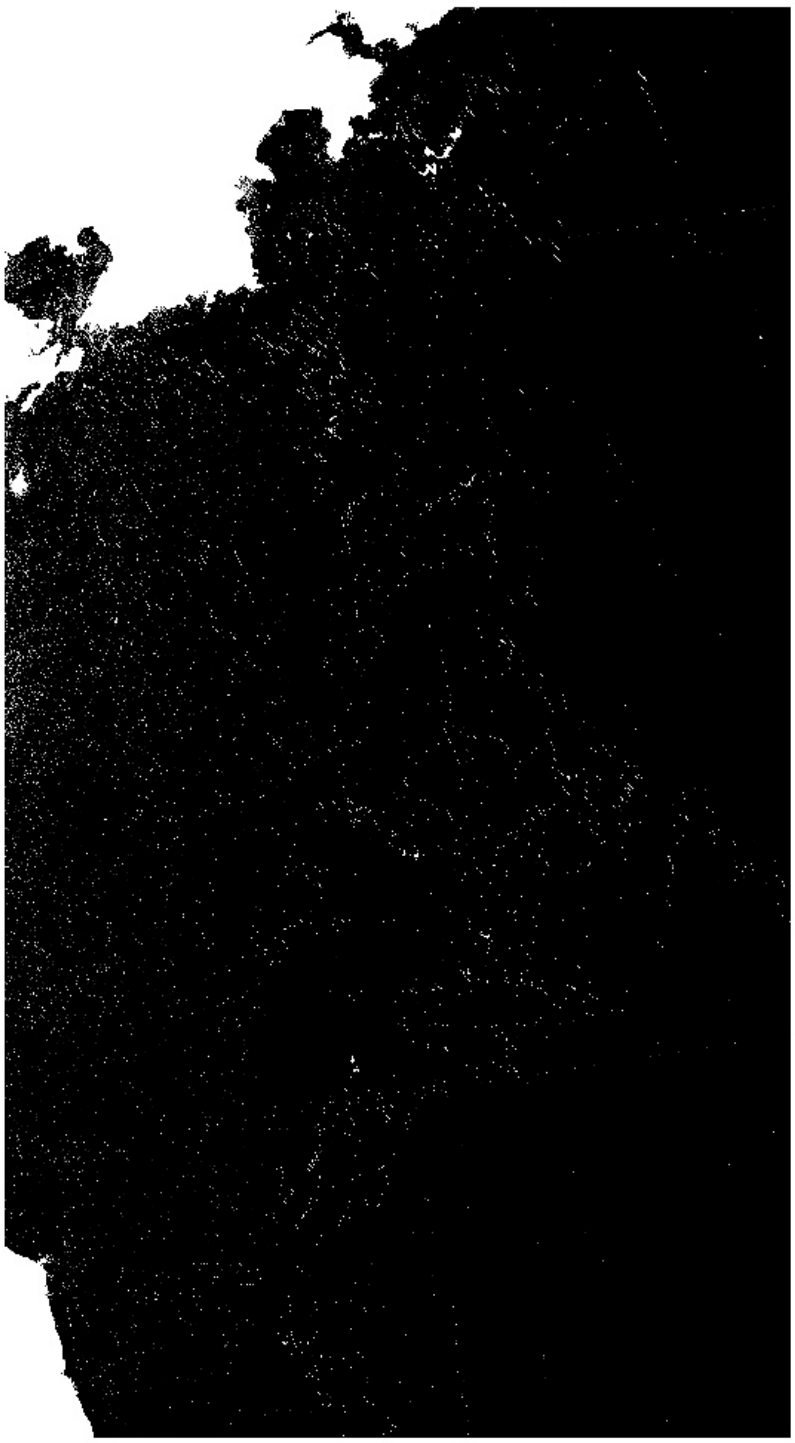

Figure 10. The result of extracting *Ulva prolifera* with a threshold of −15 dB.

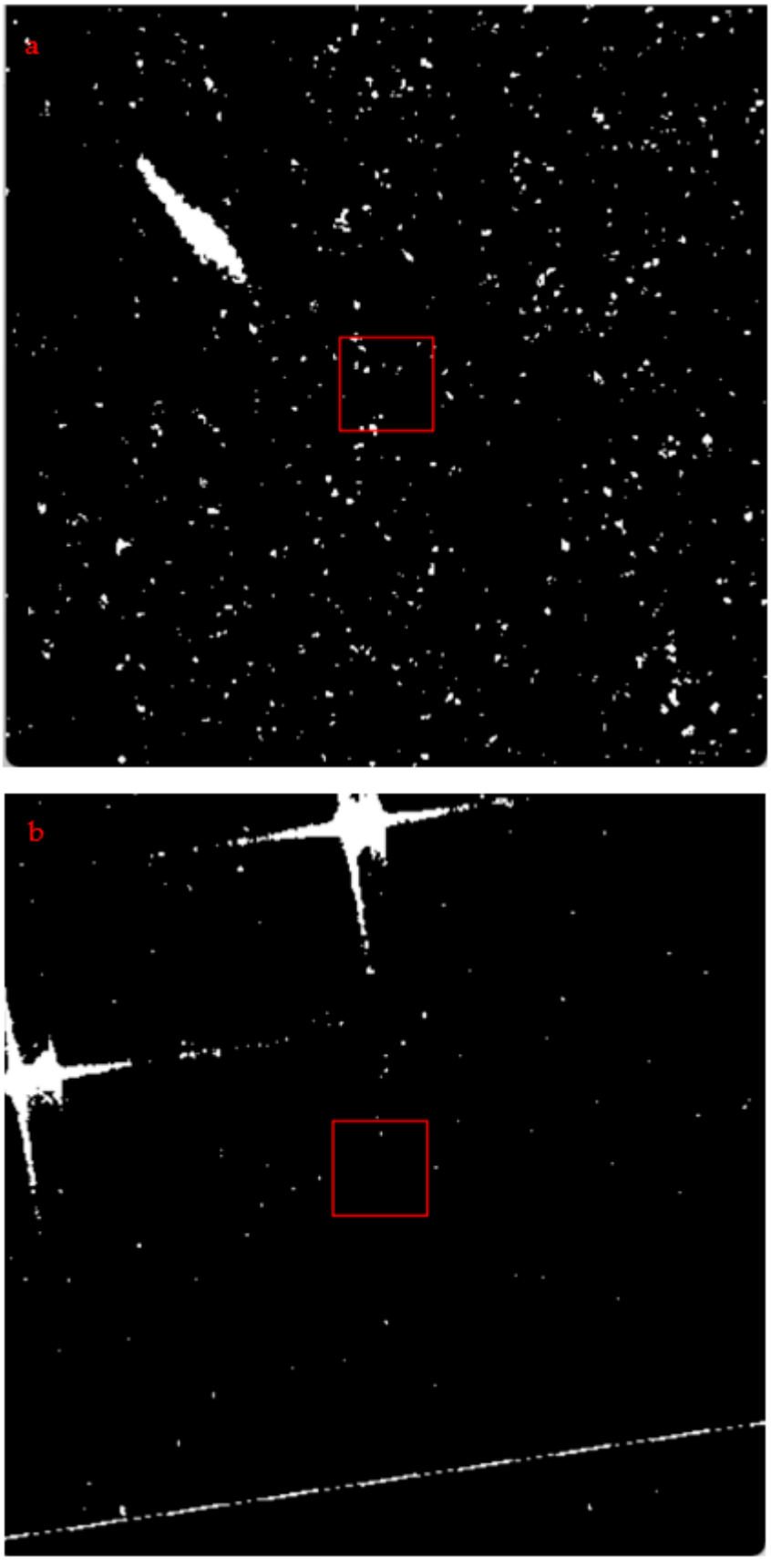

Figure 11. *Cont.*

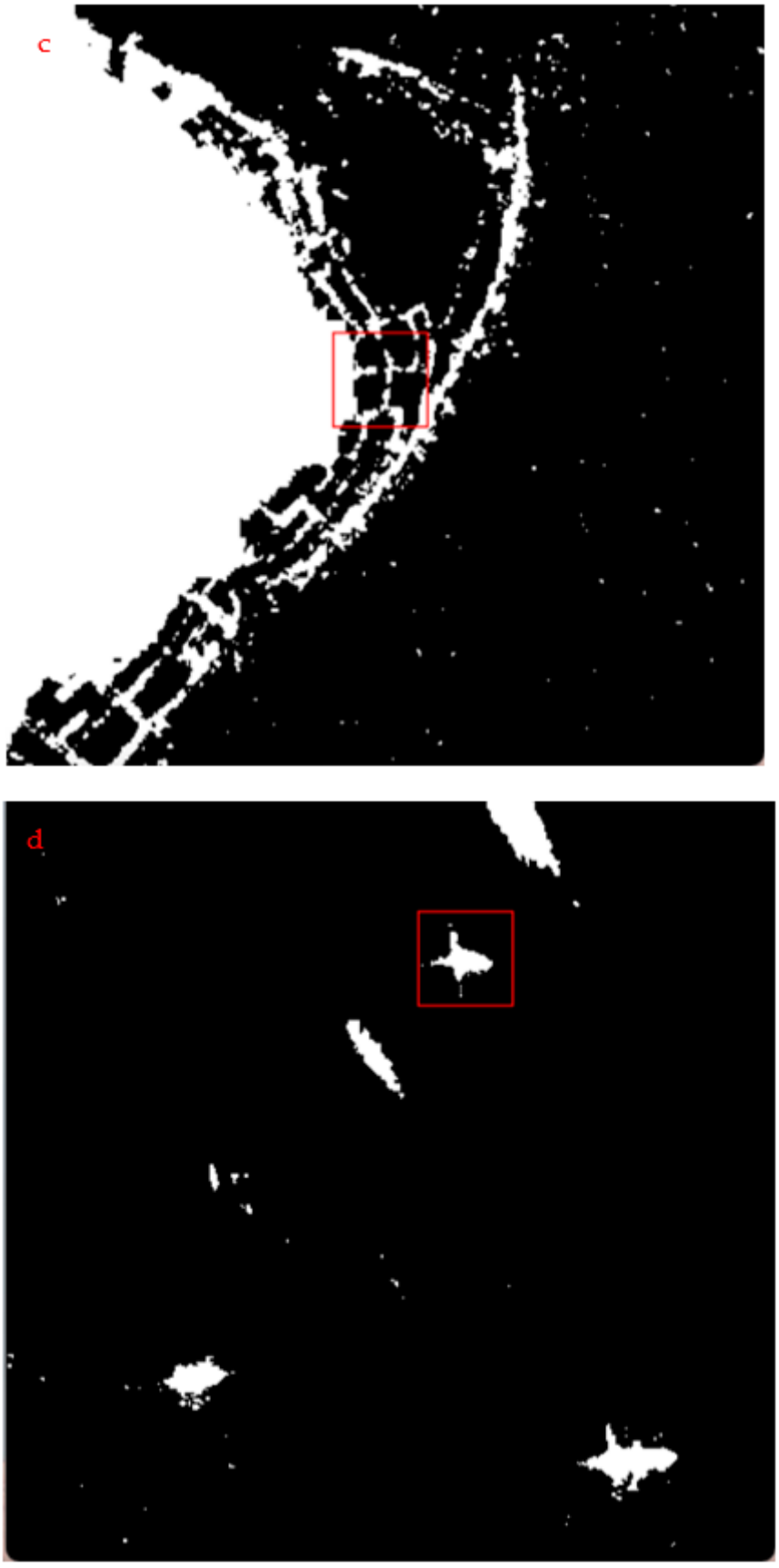

Figure 11. *Cont.*

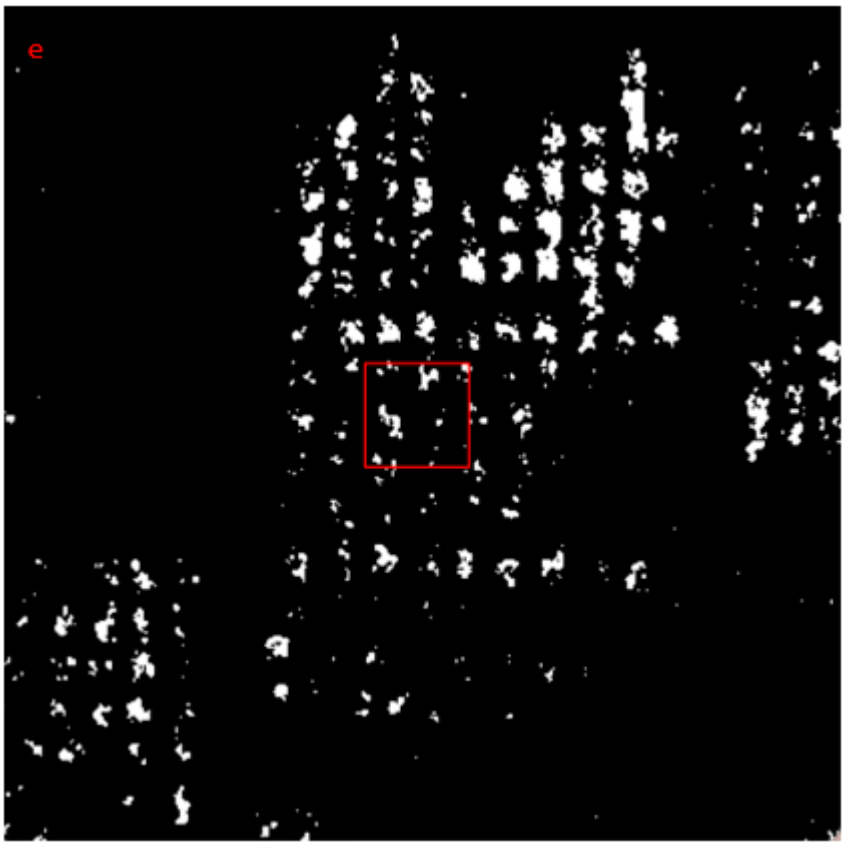

Figure 11. Non-*ulva prolifera* pixels after threshold segmentation. (**a**) Fragmented speckles; (**b**) Coherent speckle noise and splicing lines between images; (**c**) Land and coast; (**d**) Vessels; (**e**) Offshore aquaculture area.

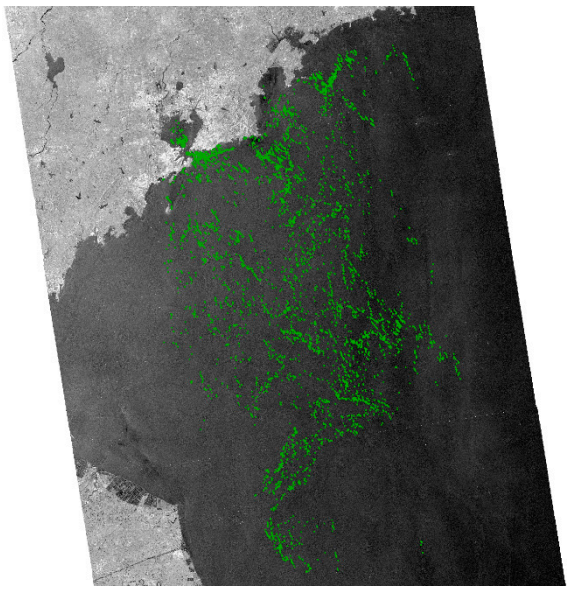

Figure 12. The extraction results of *Ulva prolifera* after removing the pixels of *Ulva prolifera*.

2.2.5. *Ulva prolifera* Drift Path and Influence Range

The *Ulva prolifera* extraction results were imported into ArcGIS10.2 and the MeanCenter tool was used to determine the center position, which represents the drift center of *Ulva prolifera*. Then the centers of *Ulva prolifera* were connected in chronological order to obtain the drifting path of *Ulva prolifera*.

The extraction area of *Ulva prolifera* is related to the spatial resolution of the data source. There are mixed pixels in any image with spatial resolution. The lower the spatial resolution, the more mixed pixels. Based on low-resolution images (especially 100 m, 250 m, and 500 m), the coverage of large algae will be overestimated [32]. Therefore, the extraction of the *Ulva prolifera* area is inconsistent. The resolution of MODIS data is 250 m, and the resolution of SAR data is 10 m. There is a big difference in the resolution of the two data points. To reflect the changes of *Ulva prolifera* more accurately and make the area of *Ulva prolifera* from these two images can be compared on the same level, the Euclidean distance method was used to extract the range of influence of *Ulva prolifera*.

Euclidean distance is the most common representation, representing the distance between two points or between multiple points. In Euclidean space, the Euclidean distance between two points an (x_1, x_2) and b (x_2, y_2) is:

$$d_{ab} = \sqrt{(x_1 - x_2)^2 + (y_1 - y_2)^2}.$$

The results of *Ulva prolifera* extraction were imported into ArcGIS, Euclidean distance analysis was used, the maximum distance to 5000 m to obtain the image after distance analysis was set, and then logical operations to convert it into a vector area were used.

3. Results

The green tide appeared along the coast of Jiangsu in May, gradually drifting northward in May and June. During the drift, the green tide continued to grow. The shape changed from a sporadic shape to a strip shape, the density increased, and the area increased. The affected seas range from the outer seas of Jiangsu to the outer seas of Shandong. *Ulva prolifera* finally landed on the coast of Qingdao. In July and August, the range of green tides gradually decreased, and the density gradually decreased.

Figure 13 shows the remote sensing monitoring results of the Yellow Sea Green Tide in 2021. MODIS observed *Ulva prolifera* for the last time on 24 May, and SAR observed *Ulva prolifera* for the final time on 11 August. The green tide duration that can be monitored by remote sensing is 80 days.

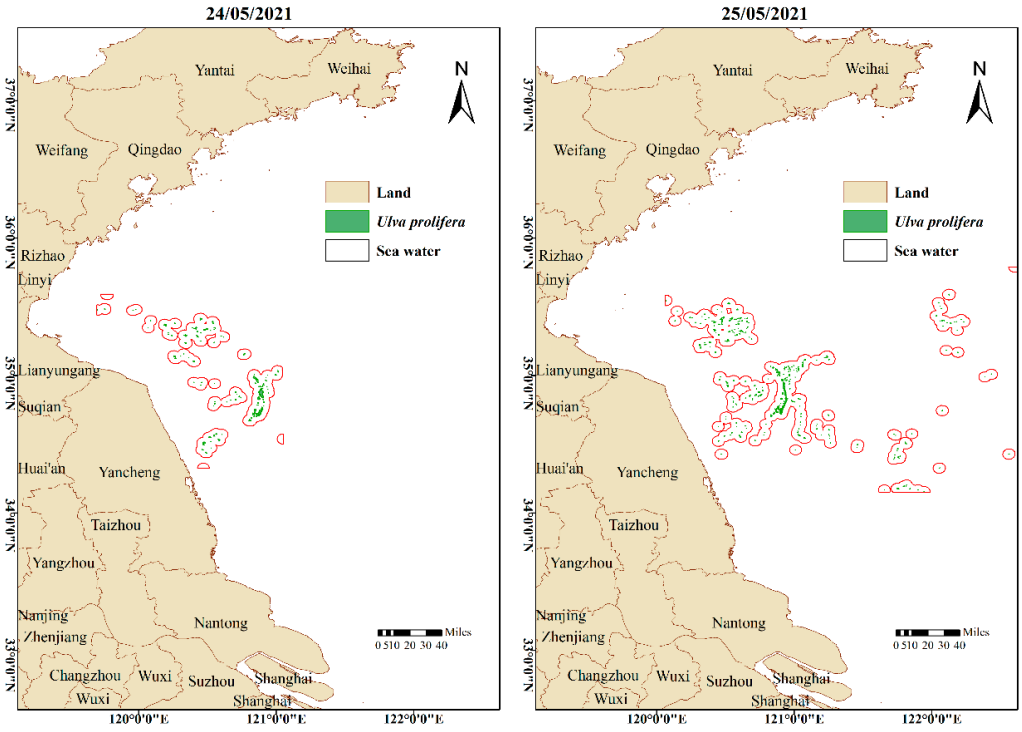

Figure 13. *Cont.*

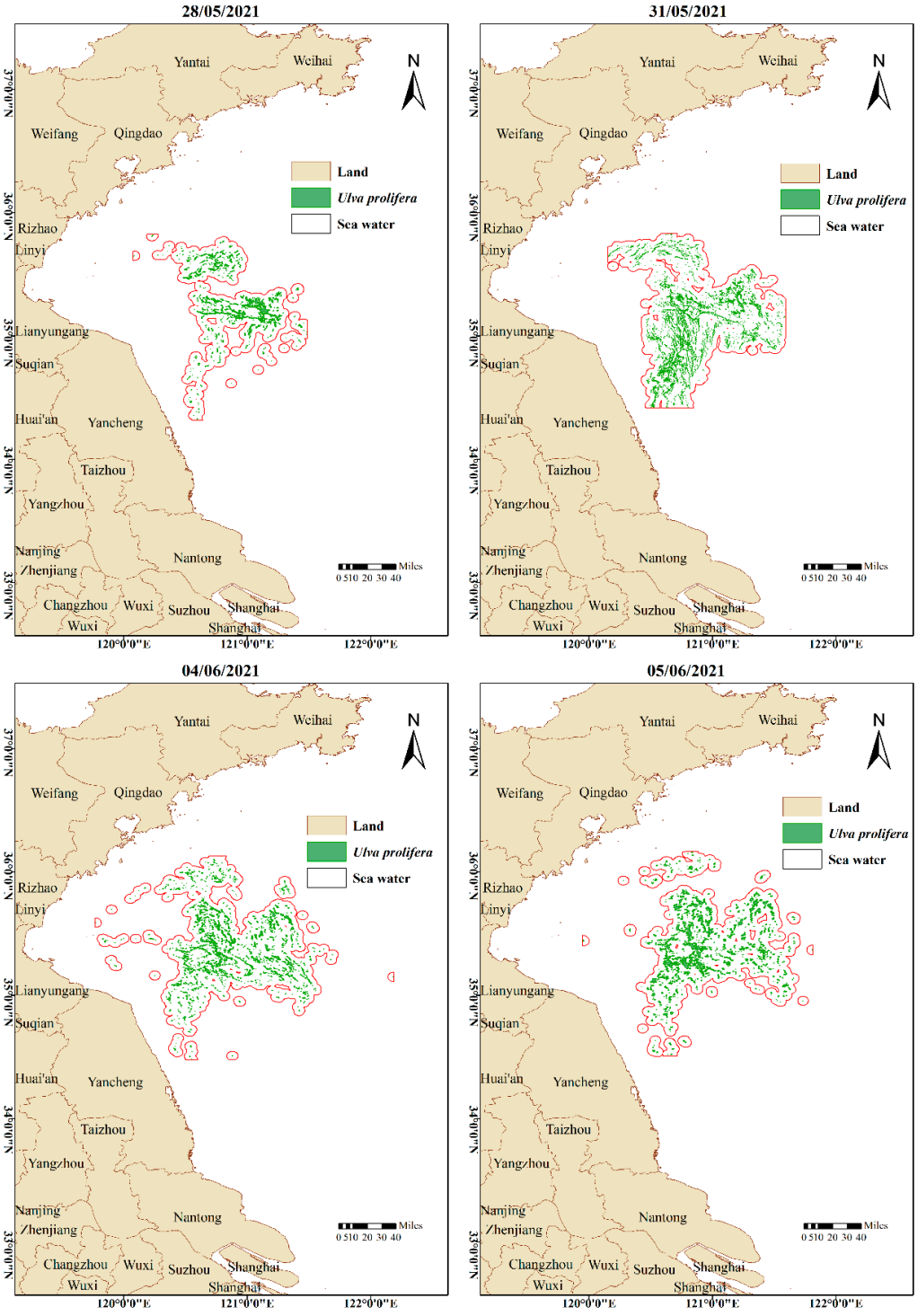

Figure 13. *Cont.*

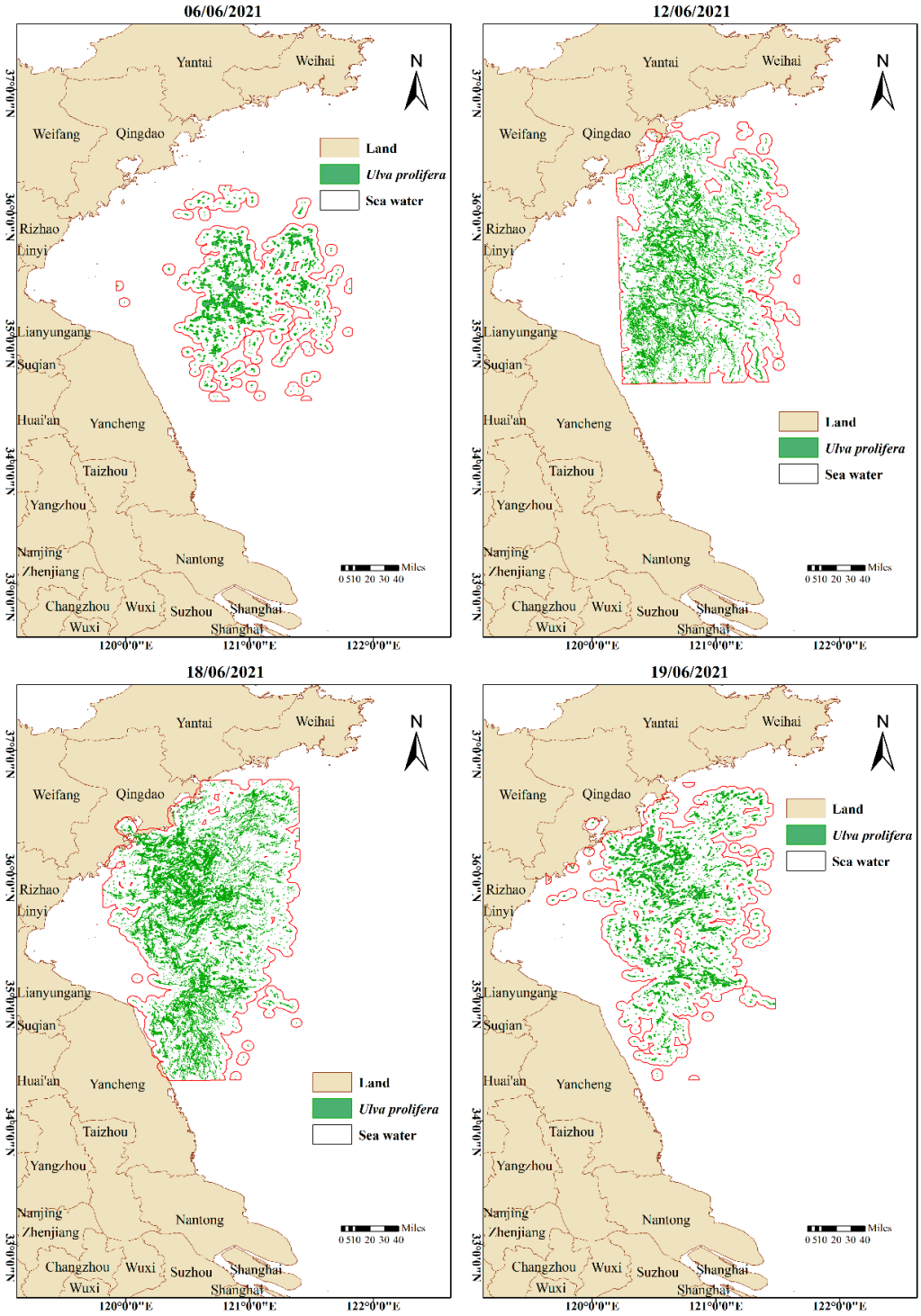

Figure 13. *Cont.*

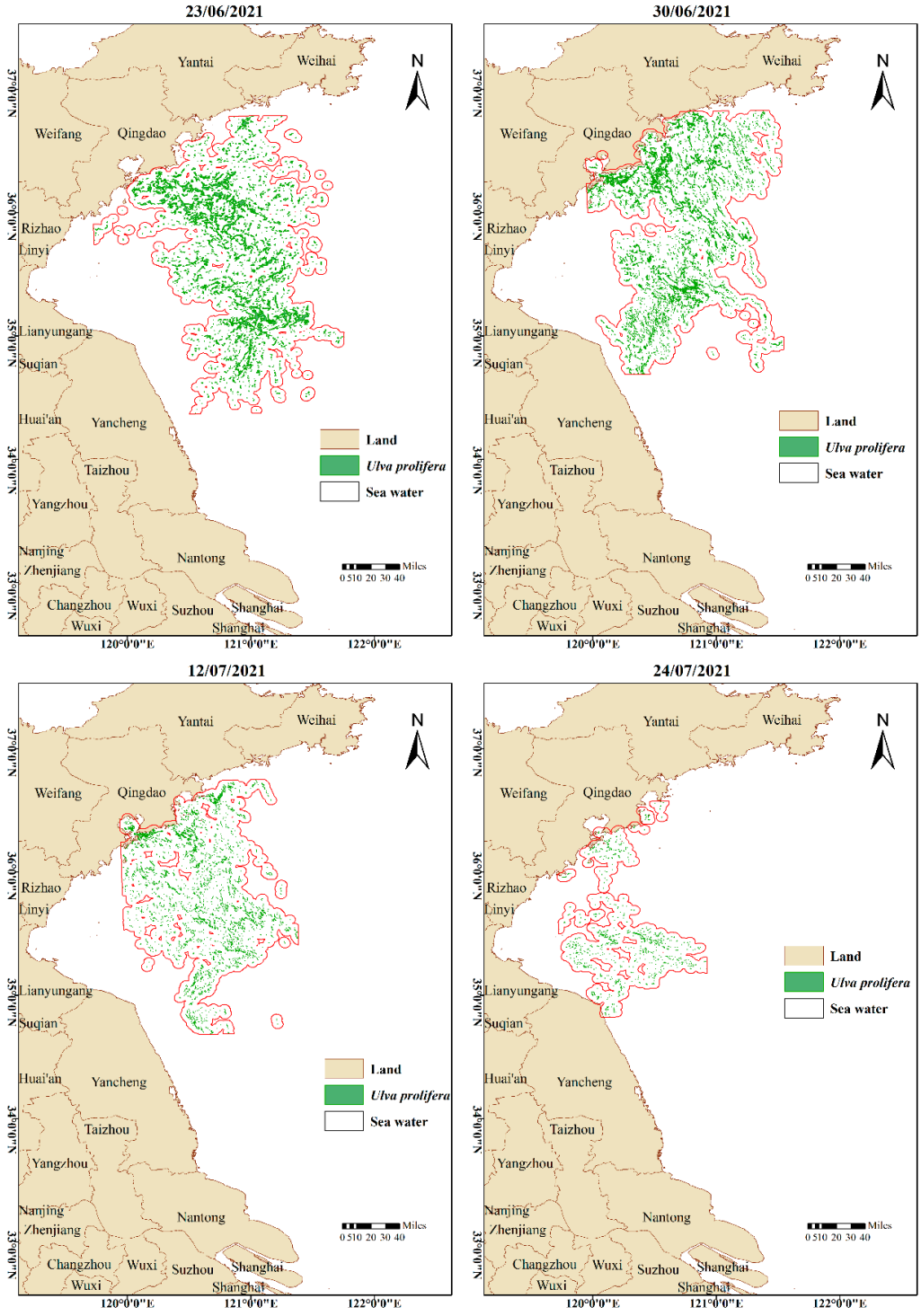

Figure 13. *Cont.*

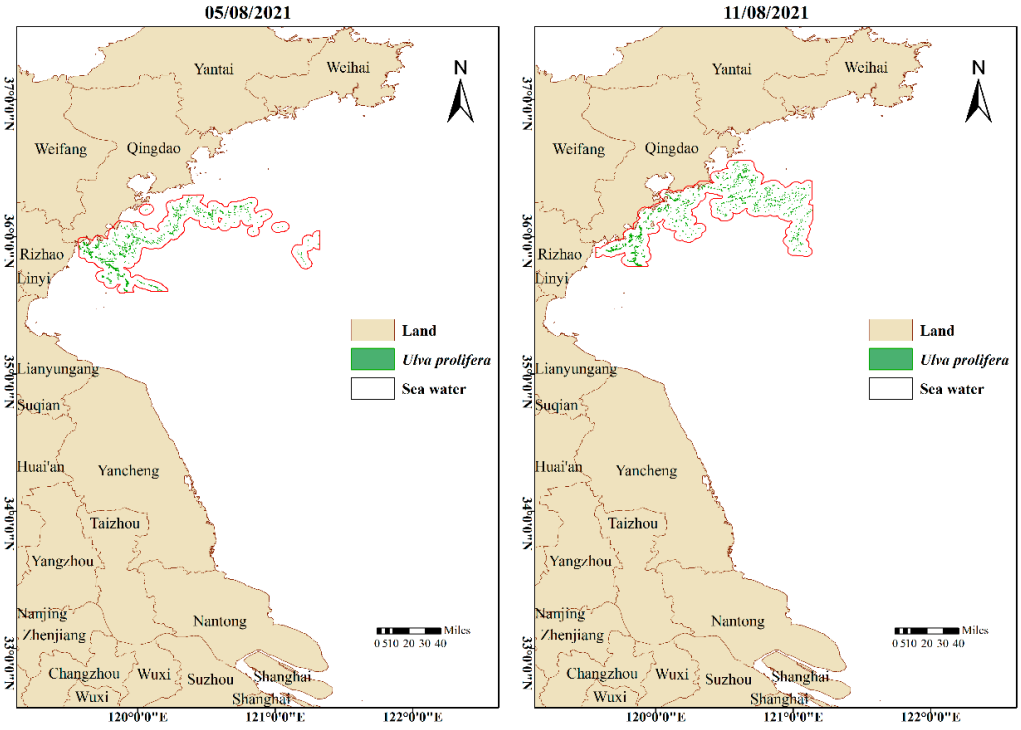

Figure 13. The thematic map of the extraction results of *Ulva prolifera* and the affected area.

On 24 May, *Ulva prolifera* appeared along the coast from Lianyungang to Yancheng. It was mainly located along the coast of Yancheng, showing small patches, scattered along the coast of Lianyungang, with a small range. On 25 May, *Ulva prolifera* along the coast increased more, and its area expanded. The concentrated *Ulva prolifera* was in the form of small strips, and some *Ulva prolifera* spread from the coast to the sea and scattered *Ulva prolifera* appeared in the open sea. *Ulva prolifera* affects the sea area extended to the waters off Lianyungang and Yancheng, but the scope of influence is relatively small. On 28 May, as the area expanded from the *Ulva prolifera* concentration area, most of *Ulva prolifera* showed a strip shape, with only the outer edge of *Ulva prolifera* scattered sporadically. After 28 May, the area continued to increase. From 31 May to 6 June, the area of *Ulva prolifera* increased slowly. During this period, the area changed little, and the banded *Ulva prolifera* gradually increased, and the whole *Ulva prolifera* drifted northward. A large area of *Ulva prolifera* appeared on 12 June. The range of *Ulva prolifera* in the north–south direction extends from the Yancheng sea area to the Qingdao sea area, and the range in the east–west direction is significantly expanded. The density of *Ulva prolifera* also increases significantly. On 18 June, the density of *Ulva prolifera* has further increased, and the range of *Ulva prolifera* has a certain extension in the north–south direction. From 19 June to 30 June, the range of *Ulva prolifera* was still in the seas from Yancheng to Qingdao, but the density gradually decreased, and the distribution range was reduced. From 30 June, the area of *Ulva prolifera* was significantly reduced. From 12 July to 11 August, the area and density of *Ulva prolifera* gradually decreased. On 5 August and 11 August, *Ulva prolifera* only appeared along the coast of Qingdao, and the *Ulva prolifera* along the coast of Jiangsu had completely disappeared.

Connect the geometric centers of *Ulva prolifera* in sequence to obtain the drifting path of *Ulva prolifera*, as shown in Figure 14. *Ulva prolifera* was first detected by satellites on 24 May, located in the northern waters of Yancheng. From 24 May to 6 June, it drifted to the open sea along the northeast direction. After 6 June, it drifted to the northwest, passing through the waters of Lianyungang, Linyi, Rizhao and Qingdao, and finally staying in the waters of Qingdao. *Ulva prolifera* tends to gather, grow and expand to the north as a whole.

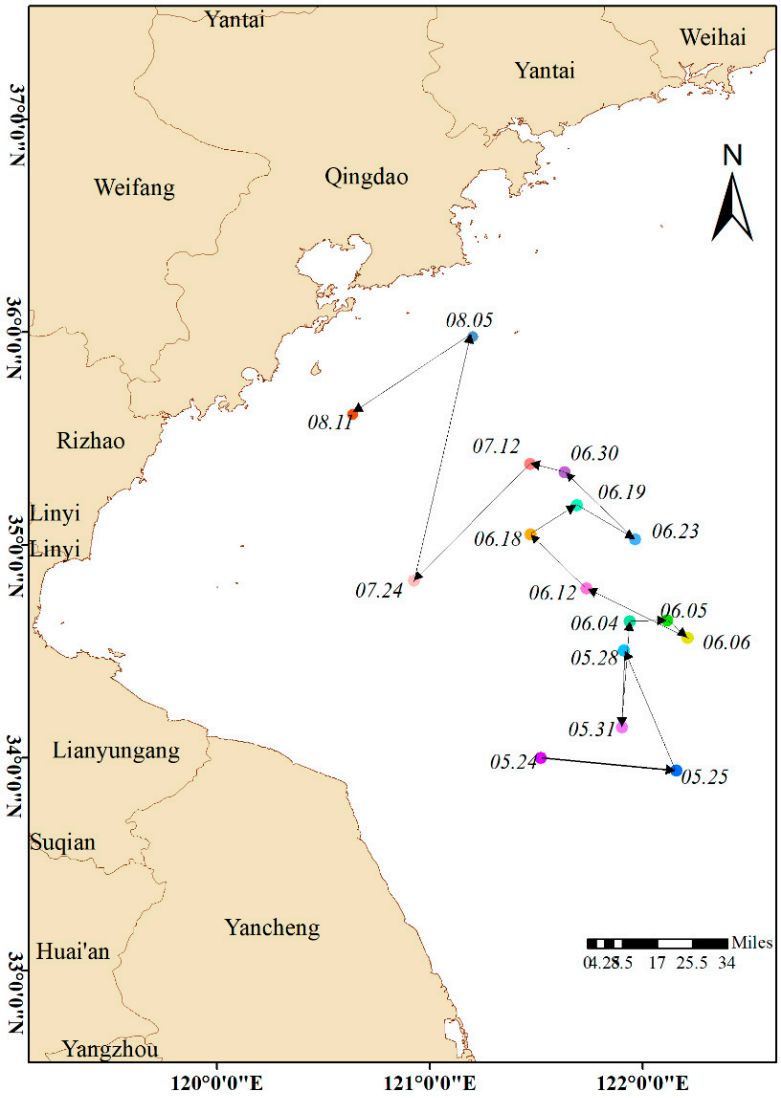

Figure 14. Thematic map of *Ulva prolifera* drift trajectory.

4. Discussion

The range enclosed by the red line in Figure 13 is the range obtained after Euclidean distance analysis is performed on the extraction results of *Ulva prolifera*, and it is taken as the range of influence of *Ulva prolifera*. Figure 15 shows the change of the influence range of *Ulva prolifera* over time. According to the size and growth rate of the influence range of *Ulva prolifera*, it is divided into five stages: "discovery-development-outbreak-decline-extinction". On 24 May, the satellite discovered *Ulva prolifera* for the first time, and its range of influence is 4346.28 km^2. It can be inferred that *Ulva prolifera* was formed in mid-to-late May. From late May to early June, the impact area of *Ulva prolifera* continues to increase, and the growth rate is the fastest at the end of May. On 6 June, the impact area of *Ulva prolifera* reached 21,062.65 km^2. From early June to mid-June, *Ulva prolifera* grows the fastest, with a sharp increase in the range of influence. It reached a peak on 18 June and the range of influence increased to 42,384.68 km^2. After late June, the range of *Ulva prolifera's* influence gradually decreased.

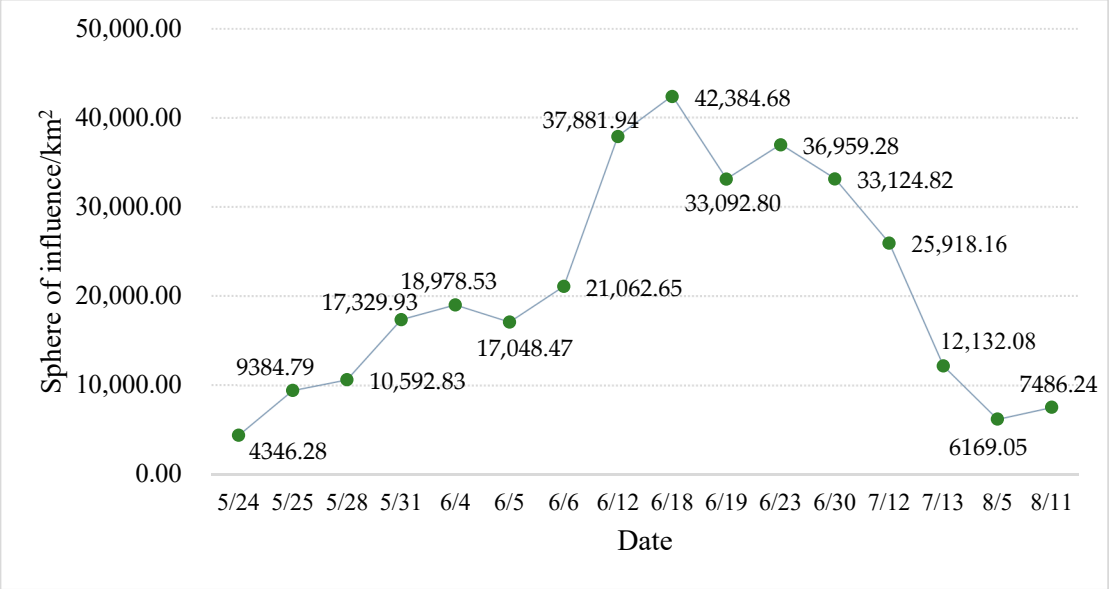

Figure 15. Changes in the influence range of *Ulva prolifera* over time.

The discovery period of *Ulva prolifera* (mid-to-late May) was in the northern waters of Yancheng; the *Ulva prolifera* development period (mid-late May to early June) mainly drifts to the open sea along the northeast direction; the *Ulva prolifera* outbreak period (from early June to mid-to-late June) drifts along the northwest direction to Qingdao sea area; the *Ulva prolifera* decay period (from late June to mid-July) did not have apparent directional drift, and was mainly located in the sea off Linyi to Rizhao; the extinction period of *Ulva prolifera* (from late July to mid-August) gradually drifted to the coast of Qingdao and landed on the coast of Rizhao and Qingdao.

5. Conclusions

In this paper, two types of remote sensing data of optical MODIS and SAR are used to jointly monitor the temporal and spatial changes of *Ulva prolifera* in the Yellow Sea in 2021. The combination of the two can effectively and accurately monitor *Ulva prolifera.*

MODIS observed *Ulva prolifera* for the first time on 24 May, whereas SAR observed *Ulva prolifera* for the last time on 11 August when it is covered by clouds. The green tide duration that can be monitored by remote sensing is 80 days. *Ulva prolifera* has undergone five development stages. The discovery period of *Ulva prolifera* is in mid-to-late May; the development period of *Ulva prolifera* is from mid-to-late June; the outbreak period of *Ulva prolifera* is from early June to mid-to-late June; the decline period of *Ulva prolifera* is from late July to mid-July; the extinction period of *Ulva prolifera* is from late July to mid-August.

The affected area of *Ulva prolifera* in the development and outbreak stages is increasing. The shape of *Ulva prolifera* in the discovery stage is scattered and dotted. The *Ulva prolifera* in the development stage is slender and striped. *Ulva prolifera* in the outbreak stage has increased dramatically as densely distributed. *Ulva prolifera* during the extinction and decline period is gradually scattered, and the area is reduced.

Ulva prolifera was located in the sea area of Yancheng during the discovery period. It first drifted in the northeast direction and entered the development period, and then drifted in the northwest direction into the outbreak period. *Ulva prolifera* had a tendency to grow northward and be densely distributed, and finally landed in the coastal waters of Rizhao and Qingdao and entered the extinction period.

Author Contributions: Conceptualization, Y.M. and Y.Z.; methodology, K.W.; software, J.Y.T.; validation, Y.M., K.W. and Y.Z.; formal analysis, Y.M.; investigation, Y.M.; resources, J.Y.T.; data curation, K.W.; writing—original draft preparation, Y.M.; writing—review and editing, K.W. and Y.Z.; visu-

alization, Y.M.; supervision, Y.Z.; project administration, Y.Z.; funding acquisition, Y.Z. All authors have read and agreed to the published version of the manuscript.

Funding: This research was funded by the Marine Special Program of Jiangsu Province in China (JSZRHYKJ202007), the National Natural Science Foundation (U1901215), and the Natural Scientific Foundation of Jiangsu Province (BK20181413).

Institutional Review Board Statement: Not applicable.

Informed Consent Statement: Not applicable.

Data Availability Statement: Not applicable.

Acknowledgments: The MODSI optical, SAR, and local yellow-book data are highly appreciated. This research was supported by the National Natural Science Foundation (U1901215), the Marine Special Program of Jiangsu Province in China (JSZRHYKJ202007), and the Natural Scientific Foundation of Jiangsu Province (BK20181413).

Conflicts of Interest: The authors declare no conflict of interest.

References

1. Leliaert, F.; Zhang, X.; Ye, N.; Malta, E.; Engelen, A.H.; Mineur, F.; Verbruggen, H.; De Clerck, O. Research note: Identity of the Qingdao algal bloom. *Psychol. Res.* **2009**, *57*, 147–151. [CrossRef]
2. Xiao, J.; Wang, Z.; Liu, D.; Fu, M.; Yuan, C.; Yan, T. Harmful macroalgal blooms (HMBs) in China's coastal water: Green and golden tides. *Harmful Algae* **2021**, *107*, 102061. [CrossRef] [PubMed]
3. Ye, N.; Zhang, X.; Mao, Y.; Liang, C.; Xu, D.; Zou, J.; Zhuang, Z.; Wang, Q. 'Green tides' are overwhelming the coastline of our blue planet: Taking the world's largest example. *Environ. Res.* **2011**, *26*, 477–485. [CrossRef]
4. Zhou, M.-J.; Liu, D.-Y.; Anderson, D.M.; Valiela, I. Introduction to the Special Issue on green tides in the Yellow Sea. *Estuar. Coast. Shelf Sci.* **2015**, *163*, 3–8. [CrossRef]
5. Pang, S.J.; Liu, F.; Shan, T.F.; Xu, N.; Zhang, Z.H.; Gao, S.Q.; Chopin, T.; Sun, S. Tracking the algal origin of the Ulva bloom in the Yellow Sea by a combination of molecular, morphological and physiological analyses. *Mar. Environ. Res.* **2010**, *69*, 207–215. [CrossRef]
6. Liu, F.; Pang, S.J.; Zhao, X.B.; Hu, C.M. Quantitative, molecular and growth analyses of Ulva microscopic propagules in the coastal sediment of Jiangsu province where green tides initially occurred. *Mar. Environ. Res.* **2012**, *74*, 56–63. [CrossRef]
7. Zong, L. A Preliminary Study of the Enteromorpha prolifera Drift Gathering Causing the Green Tide Phenomenon. *Period. Ocean Univ. China* **2008**, *38*, 601–604.
8. Zhang, X.; Xu, D.; Mao, Y.; Li, Y.; Xue, S.; Zou, J.; Lian, W.; Liang, C.; Zhuang, Z.; Wang, Q.; et al. Settlement of vegetative fragments of Ulva prolifera confirmed as an important seed source for succession of a large-scale green tide bloom. *Limnol. Oceanogr. Lett.* **2010**, *56*, 233–242. [CrossRef]
9. Liu, D.; Keesing, J.K.; Dong, Z.; Zhen, Y.; Di, B.; Shi, Y.; Fearns, P.; Shi, P. Recurrence of the world's largest green-tide in 2009 in Yellow Sea, China: Porphyra yezoensis aquaculture rafts confirmed as nursery for macroalgal blooms. *Mar. Pollut. Bull.* **2010**, *60*, 1423–1432. [CrossRef]
10. Liu, D.; Keesing, J.K.; He, P.; Wang, Z.; Shi, Y.; Wang, Y. The world's largest macroalgal bloom in the Yellow Sea, China: Formation and implications. *Estuar. Coast. Shelf Sci.* **2013**, *129*, 2–10. [CrossRef]
11. Wang, Z.; Xiao, J.; Fan, S.; Li, Y.; Liu, X.; Liu, D. Who made the world's largest green tide in China?—An integrated study on the initiation and early development of the green tide in Yellow Sea. *Limnol. Oceanogr.* **2015**, *60*, 1105–1117. [CrossRef]
12. Zhou, R.; Sha, J.; Wen, R.; Li, J.; Pan, Y.; Wei, M.; Wang, H.; Wang, T.; Zhang, J.; Zhao, S. Present situation and prospect of green tide monitoring technology. *IOP Conf. Ser. Earth Environ. Sci.* **2021**, *769*, 032043. [CrossRef]
13. Qiu, Y.H.; Lu, J.B. Advances in the monitoring of Enteromorpha prolifera using remote sensing. *Acta Ecol. Sin.* **2015**, *35*, 4977–4985.
14. Hu, C.; He, M.X. Origin and offshore extent of floating algae in olympic sailing area. *Eos Trans. Am. Geophys. Union* **2008**, *89*, 302–303. [CrossRef]
15. Jia, L.; Zhang, A.; Wu, M. Spatial and temporal distribution characteristic of Enteromorpha in Shandong Peninsula in 2013 on the Basis of MODIS Data. *Yantai Teach. Univ. J. Nat. Sci. Ed.* **2015**, *2*, 172–177.
16. Shen, H.; Lu, R.; Li, D. Remote sensing of the Yellow Sea green tide evolution in 2015. *Mar. Sci.* **2016**, *40*, 134–142.
17. Han, J.; Huang, H.; Zhang, W.; Lin, W. Distribution characteristics and dynamic mechanism of Enteromorpha prolifera in the Yellow Sea in 2018. *Mar. Sci.* **2020**, *44*, 37–44.
18. Song, D.-B.; Gao, Z.-Q.; Xu, F.-X.; Ai, J.-Q.; Ning, J.-C.; Shang, W.-T.; Jiang, X.-P. Spatial and temporal variability of the green tide in the south Yellow Sea in 2017 deciphered from the GOCI image. *Oceanol. Limnol. Sin.* **2018**, *49*, 1068–1074.
19. Chen, Y.; Sun, D.; Zhang, H.; Wang, S.; Qiu, Z.; He, Y. Remote-sensing monitoring of green tide and its drifting trajectories in Yellow Sea Based on observation data of geostationary ocean color imager. *Acta Opt. Sin.* **2020**, *40*, 7–19.
20. Wu, C.Q.; Ma, W.D.; Wang, X.L.; Yao, Y.J.; Wu, D. Remote Sensing Monitoring Hab in Yellow Sea by HJ1-CCD. *Environ. Monit. China* **2015**, *31*, 161–165.

21. Zhang, H.; Sun, D.; Li, J.; Qiu, Z.; Wang, S.; He, Y. Remote sensing algorithm for detecting green tide in china coastal waters based on GF1-WFV and HJ-CCD data. *Acta Opt. Sin.* **2016**, *36*, 0601004. [CrossRef]
22. Yuan, H.; Wu, C.; Lu, L.; Wang, X. A new algorithm predicting the end of growth at five evergreen conifer forests based on nighttime temperature and the enhanced vegetation index. *ISPRS J. Photogramm. Remote Sens.* **2018**, *144*, 390–399. [CrossRef]
23. Cao, Y.; Wu, Y.; Fang, Z.; Cui, X.; Liang, J.; Song, X. Spatiotemporal patterns and morphological characteristics of ulva prolifera distribution in the Yellow Sea, China in 2016–2018. *Remote Sens.* **2019**, *11*, 445. [CrossRef]
24. Gupta, R.K.; Prasad, S.; Nadham, T.S.V.; Rao, G.H. Relative sensitivity of district mean RVI and NDVI over an agrometeorological zone. *Adv. Space Res.* **1993**, *13*, 261–264. [CrossRef]
25. Wang, Z.; Fang, Z.; Wu, Y.; Liang, J.; Song, X. Multi-source evidence data fusion approach to detect daily distribution and coverage of Ulva prolifera in the Yellow Sea, China. *IEEE Access* **2019**, *7*, 115214–115228. [CrossRef]
26. Hu, C. A novel ocean color index to detect floating algae in the global oceans. *Remote Sens. Environ.* **2009**, *113*, 2118–2129. [CrossRef]
27. Xing, Q.; Hu, C. Mapping macroalgal blooms in the Yellow Sea and East China Sea using HJ-1 and Landsat data: Application of a virtual baseline reflectance height technique. *Remote Sens. Environ.* **2016**, *178*, 113–126. [CrossRef]
28. Shi, W.; Wang, M. Green macroalgae blooms in the Yellow Sea during the spring and summer of 2008. *J. Geophys. Res.* **2009**, *114*. [CrossRef]
29. Ciappa, A.; Pietranera, L.; Coletta, A.; Jiang, X. Surface transport detected by pairs of COSMO-SkyMed ScanSAR images in the Qingdao region (Yellow Sea) during a macro-algal bloom in July 2008. *J. Mar. Syst.* **2010**, *80*, 135–142. [CrossRef]
30. Jiang, X.; Zou, Y.; Wang, H.; Zhu, H. Application study on quick extraction of Entermorpha prolifera information using SAR data. *Acta Oceanol. Sin.* **2009**, *31*, 63–68.
31. Shen, H.; Perrie, W.; Liu, Q.; He, Y. Detection of macroalgae blooms by complex SAR imagery. *Mar. Pollut. Bull.* **2014**, *78*, 190–195. [CrossRef] [PubMed]
32. Wang, X.; Xing, Q.; An, D.; Meng, L.; Zheng, X.; Jiang, B.; Liu, H. Effects of Spatial Resolution on the Satellite Observation of Floating Macroalgae Blooms. *Water* **2021**, *13*, 1761. [CrossRef]